

This work was written as part of one of the author's official duties as an Employee of the United States Government and is therefore a work of the United States Government. In accordance with 17 U.S.C. 105, no copyright protection is available for such works under U.S. Law.

Public Domain Mark 1.0

<https://creativecommons.org/publicdomain/mark/1.0/>

Access to this work was provided by the University of Maryland, Baltimore County (UMBC) ScholarWorks@UMBC digital repository on the Maryland Shared Open Access (MD-SOAR) platform.

**Please provide feedback**

Please support the ScholarWorks@UMBC repository by emailing [scholarworks-group@umbc.edu](mailto:scholarworks-group@umbc.edu) and telling us what having access to this work means to you and why it's important to you. Thank you.

## Three Dimensional Anisotropic $k$ Spectra of Turbulence at Subproton Scales in the Solar Wind

F. Sahraoui\*

*Laboratoire de Physique des Plasmas, CNRS-Ecole Polytechnique-UPMC, Observatoire de Saint-Maur, 4 avenue de Neptune, 94107 Saint-Maur-des-Fossés, France*

M. L. Goldstein

*NASA Goddard Space Flight Center, Code 673, Greenbelt, Maryland 20771, USA*

G. Belmont, P. Canu, and L. Rezeau

*Laboratoire de Physique des Plasmas, CNRS-Ecole Polytechnique-UPMC, Route de Saclay, 91128 Palaiseau, France*

(Received 14 May 2010; published 23 September 2010; publisher error corrected 27 September 2010)

We show the first three dimensional (3D) dispersion relations and  $k$  spectra of magnetic turbulence in the solar wind at subproton scales. We used the Cluster data with short separations and applied the  $k$ -filtering technique to the frequency range where the transition to subproton scales occurs. We show that the cascade is carried by highly oblique kinetic Alfvén waves with  $\omega_{\text{plas}} \leq 0.1 \omega_{\text{ci}}$  down to  $k_{\perp} \rho_i \sim 2$ . Each  $k$  spectrum in the direction perpendicular to  $\mathbf{B}_0$  shows two scaling ranges separated by a breakpoint (in the interval  $[0.4, 1]k_{\perp} \rho_i$ ): a Kolmogorov scaling  $k_{\perp}^{-1.7}$  followed by a steeper scaling  $\sim k_{\perp}^{-4.5}$ . We conjecture that the turbulence undergoes a *transition range*, where part of the energy is dissipated into proton heating via Landau damping and the remaining energy cascades down to electron scales where electron Landau damping may predominate.

DOI: 10.1103/PhysRevLett.105.131101

PACS numbers: 96.60.Vg, 52.35.Ra, 94.05.Lk, 95.30.Qd

Large scale solar wind (SW) turbulence, where the MHD approximation is valid, has been extensively studied over the past decades, both observationally and theoretically. A general consensus exists that turbulence at those scales is dominated by strongly nonlinear Alfvén waves, yielding power law spectra with the Kolmogorov scaling  $k^{-5/3}$  [1–5]. In contrast, electron scales have been only recently explored by using data from the four Cluster satellites [6]. The first evidence of dispersion and dissipation ranges of SW turbulence at electron scales was reported in Ref. [7], which was confirmed later in other studies [8,9]. Despite this significant progress, a strong debate continues as to the actual nature of the turbulence in this region of the spectrum, i.e., whether or not it is kinetic Alfvén waves (KAW) [2,7] or whistler [10,11] turbulence. This is a key question that relates directly to the problem of plasma heating and particle acceleration in astrophysics [12]. The difficulty in addressing this problem unambiguously stems from the lack of direct measurements of full 3D dispersion relations at small scales. Indeed, nearly all previous research has used additional assumptions, such as the Taylor frozen-in-flow approximation [13], to infer the spatial properties of the turbulence from the measured temporal ones. The Taylor assumption is valid only if all fluctuation phase speeds are smaller than the flow speed  $V_f$ . This assumption is likely to break down for whistler waves and other dispersive fluctuations whose phase speed increases with wave number. More importantly, this assumption provides only the wave number

spectrum in the direction parallel to the flow. The absence of information on the two other directions prevents a full estimation of the dispersion relations, which compromises the chance of identifying unambiguously the nature of small scale turbulence.

In this Letter, we present a partial solution to this problem by computing, for the first time, the 3D dispersion relation and  $k$  spectra at both proton and subproton scales in the SW by using the  $k$ -filtering technique on Cluster data. This technique allows us, by using data recorded simultaneously in different points of space, to estimate the spectral power in both frequency and wave number,  $P(\omega, \mathbf{k})$ , under the assumption that the time series are at least weakly stationary [14]. The technique has been used successfully in the magnetosphere [15–20] and more recently in the SW where anisotropic spectra of MHD turbulence have been obtained [5].

The data used here were recorded in the SW on 10 January 2004 from 06h05 to 06h55 UT. This time interval is a rare sample that fulfills the requirements needed for the present study: (i) The spacecraft were located in the SW without connection to electron foreshock; (ii) burst mode data were available (with a sampling 450 Hz), which allows examination of high frequency turbulence; (iii) the magnetic fluctuations had high amplitudes relative to the sensitivity floor of the Cluster Search-Coil magnetometer (STAFF-SC) [6,7]; (iv) the Cluster spacecraft formed a regular tetrahedron configuration, a *necessary* condition for appropriate  $k$ -spectra determina-

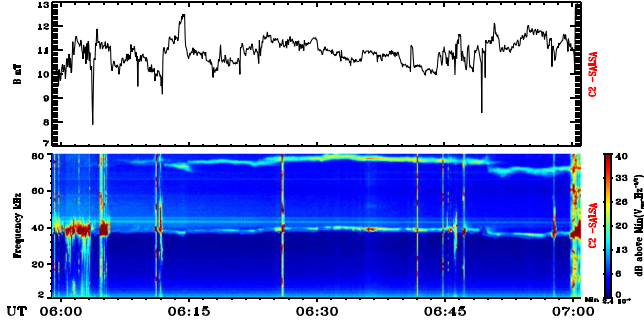


FIG. 1 (color online). Magnetic field data from FGM (top) and the plasma frequency as detected by the waves of high frequency and sounder for probing of electron density by relaxation experiment instrument (bottom) on board Cluster 2.

tion [21]; (v) the spacecraft separation ( $d \sim 200$  km) was appropriate for exploring subproton scales.

Figure 1 shows the magnetic field measured by the flux gate magnetometer (FGM) and the plasma frequency measured by the waves of high frequency and sounder for probing of electron density by relaxation experiment [6]. We use the latter to select periods of time where the SW is not connected to the terrestrial electron foreshock (Table I). We have also avoided as much as possible sharp gradients in the magnetic field components.

Figure 2 shows the Fourier power spectra of  $B_{\parallel}$  and  $B_{\perp}$  for one time interval ( $\parallel$  and  $\perp$  denote the parallel and perpendicular directions to the mean field  $\mathbf{B}_0$ , respectively). These spectra and those computed from the other time intervals of Table I (not shown here) show very similar features to those reported by Refs. [7,9], viz., a Kolmogorov scaling  $f^{-1.7}$  at large scale, a breakpoint around the proton gyroscale (rather than the proton gyrofrequency  $f_{ci}$ ), a new inertial range at subproton scales with a power law  $\sim f^{-2.8}$  followed by a second breakpoint, and a steepening around the electron gyroscale or inertial length (here the second breakpoint is less visible on the parallel component of the fluctuations). A careful investigation of these spectra show an interesting feature: Right above the breakpoint at the proton scale the spectrum actually

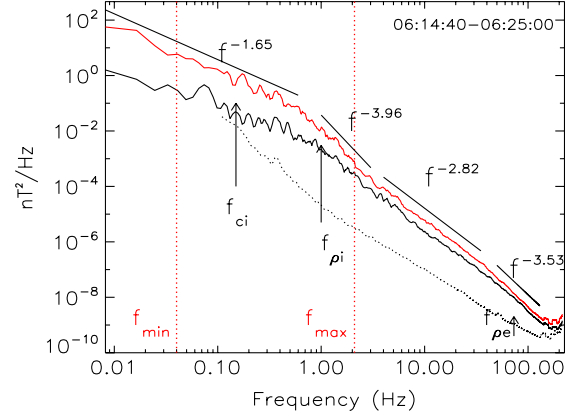


FIG. 2 (color online). Parallel (black curve) and perpendicular (red curve) power spectra from FGM ( $f < 2$  Hz) and STAFF-SC ( $f > 2$  Hz) data. The black dotted line is the in-flight sensitivity floor of STAFF-SC. Vertical arrows are the proton gyrofrequency  $f_{ci}$  and the ‘‘Doppler-shifted’’ proton and electron gyro radii ( $f_{\rho} = V_f/2\pi\rho$ ). The vertical dotted lines delimit the interval  $[f_{\min}, f_{\max}]$  accessible to analysis by using the  $k$ -filtering technique.

steepens to  $\sim f^{-4}$  up to  $f_{sc} \sim 3$  Hz where a transition to dispersive cascade occurs.

Figure 3 shows the power spectra of  $B_z$  in the satellite spin reference frame (despun inverted system of reference). This component is not contaminated by the effect of the satellite spin (at 0.25 Hz), which allows for good cross-checking of the two spectra to the cutoff frequency 0.1 Hz of STAFF-SC. Figure 3 shows good matching of the two spectra in the interval [0.2, 3] Hz, and both give evidence of the strong steepening above the proton breakpoint. Most likely, it is this *transition range* [22] that has been attributed in earlier work to damping of oblique propagating KAWs [23,24] or to proton cyclotron heating [25–28]. Below, we show indeed that this steepening is likely to heat protons *but* rather via Landau damping and that the residual energy continues its cascade to electron scales where it may be dissipated via electron Landau damping [12].

TABLE I. Average plasma parameters during the selected time periods (cluster ion spectrometry experiment and plasma electron and current experiment data were used [6]).

	06:06–06:10	06:15–06:25	06:27–06:41	06:50–06:55
$B$ (nT)	10	10.2	10.7	10.8
$N$ ( $\text{cm}^{-3}$ )	16	16	15	14
$T_i; T_e$ (eV)	31; 10	31; 10.4	29; 10	30; 10
$V_f$ (km/s)	547	548	561	546
$\Theta_{BV_f}$ ( $^{\circ}$ )	59	67	92	64
$f_{ci}$ (Hz)	0.15	0.15	0.16	0.16
$V_A$ (km/s)	55	58	59	63
$V_{th_i}$ (km/s)	77	76	74	75
$d_i^a; \rho_i$ (km)	59; 80	62; 76	61; 74	65; 76
$\beta_i$	1.9	1.7	1.6	1.4

<sup>a</sup>Proton inertial length.

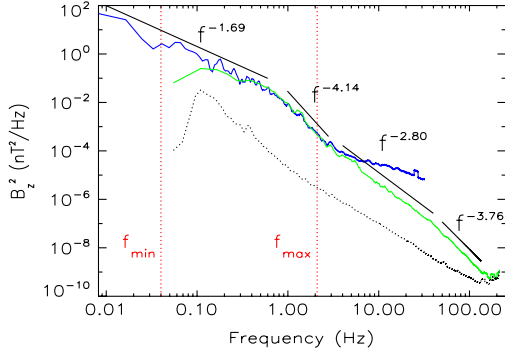


FIG. 3 (color online).  $B_z$  spectra measured by FGM (blue curve) and STAFF-SC (green curve) in the despun inverted system of reference from 06:15 to 06:25 (flattening for  $f \geq 3$  Hz is due to hitting the noise floor of the FGM). The black dotted line is the in-flight sensitivity floor of STAFF-SC.

To determine unambiguously the nature of the turbulence and its anisotropies, we apply the  $k$ -filtering technique to each frequency in the interval  $[f_{\min}, f_{\max}] \sim [0.04, 2]$  Hz in Fig. 2. The limit  $f_{\max}$  is imposed by the need to limit spatial aliasing, while  $f_{\min}$  is fixed so that the wave vectors are determined with an accuracy better than 15% [21]. By estimating the full wave vector(s) for each frequency  $f_{\text{sc}}$ , one can transform the quantity  $P(\omega_{\text{sc}}, \mathbf{k})$  into  $P(\omega_{\text{plas}}, \mathbf{k})$  after correcting for the Doppler shift  $\omega_{\text{plas}} = \omega_{\text{sc}} - \mathbf{k} \cdot \mathbf{V}_f$ . The quantity  $P(\omega_{\text{plas}}, \mathbf{k})$  can then be used to obtain both the dispersion relation  $\omega_{\text{plas}} = \omega_{\text{plas}}(\mathbf{k})$  and the integrated spectra  $P^*(\mathbf{k}) = \int P(\omega_{\text{plas}}, \mathbf{k}) d\omega_{\text{plas}}$ . Both quantities can be compared directly to theoretical predictions so as to determine unambiguously the actual nature of the turbulence.

Figure 4 shows clearly that the wave vectors are highly oblique with respect to  $\mathbf{B}_0$ ,  $\langle \Theta_{\mathbf{kB}} \rangle \sim 88^\circ$ . The slight departure from this value at low frequency is due to a larger uncertainty ( $\sim 15^\circ$ ) at large scales [21]. This result proves that the turbulence is strongly anisotropic (i.e.,  $k_{\parallel} \ll k_{\perp}$ ). The wave vectors form moderate angles with the SW flow,  $\langle \Theta_{\mathbf{kV}_f} \rangle \sim 40^\circ$  (results from the third time interval are

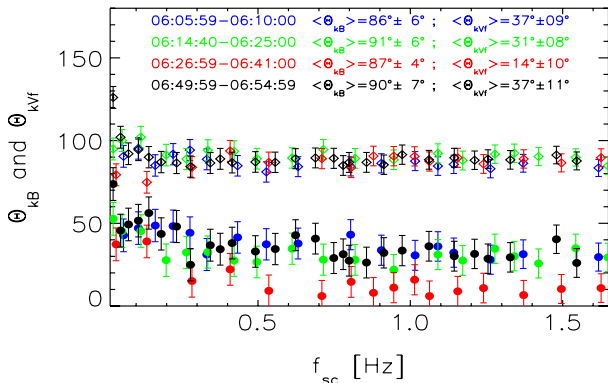


FIG. 4 (color online). Angles  $\Theta_{\mathbf{kB}}$  (diamonds) and  $\Theta_{\mathbf{kV}_f}$  (dots) with related error bars as estimated by using the  $k$ -filtering technique.

slightly different and show a quasialignment with the flow). The finite angles  $\Theta_{\mathbf{kV}_f}$  and their relative variation with frequency might lead to significant distortions in the  $k$  spectra if they were computed by using the Taylor frozen-in-flow approximation [4,29].

Figure 5 displays the observed dispersion relations compared to linear solutions of the Maxwell-Vlasov equations, calculated by using the observed plasma parameters of Table I. In addition to the uncertainty in the wave vector determination [18,21], we used 10% uncertainty on the flow to estimate the error bars plotted in this figure [16]. We can see clearly that the turbulence cascades following the KAW mode in the scale range  $[0.04, 2]k_{\perp}\rho_i$ , covering both the transition and the Kolmogorov inertial ranges, where the proton Landau damping dominates over the electron Landau and proton cyclotron dampings. The observed dispersion relations lie in the diagram far from the curve of the fast magnetosonic mode. We recall that, in a hot plasma (here  $\beta_i \sim 1.7$ ) and highly oblique propagation, the fast mode is modified by the gyroresonances, splitting into the different branches of Bernstein modes [30]. Whether the turbulence remains quasistationary (i.e.,  $\omega \ll \omega_{\text{ci}}$ ) for scales  $k_{\perp}\rho_i \gg 1$ , as suggested in Ref. [7], or develops high frequency fluctuations ( $\omega \sim \omega_{\text{ci}}$ ), requires probing to much smaller scales than those studied here. This, unfortunately, cannot be done with the available data (this regime should be observable by, e.g., the magnetospheric multiscale mission). An immediate consequence of these results is that the damping of turbulence and heating of the protons will arise most likely via Landau damping and not by cyclotron resonances [25,26,31].

Figure 6 shows the  $k$  spectra integrated over the temporal frequencies  $\omega_{\text{plas}}$  [5,18] (see [21] for details). The spectra show that the turbulence cascades perpendicularly

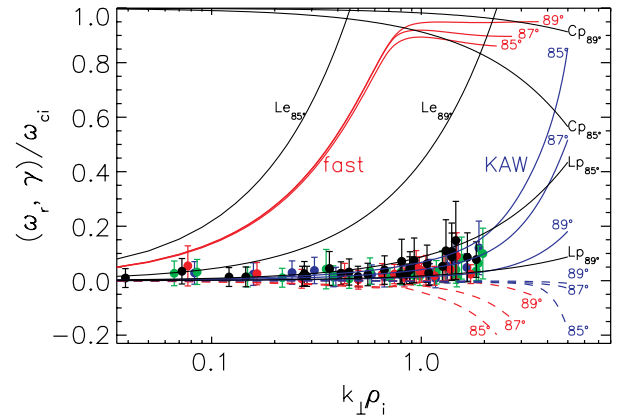


FIG. 5 (color online). Observed dispersion relations (dots), with estimated error bars, compared to linear solutions of the Maxwell-Vlasov equations for three observed angles  $\Theta_{\mathbf{kB}}$  (the dashed lines are the damping rates). The black curves ( $L_{p,e}$ ) are the proton and electron Landau resonances  $\omega = k_{\parallel}V_{thi,e}$ , and the curves  $C_p$  are the proton cyclotron resonance  $\omega = \omega_{\text{ci}} - k_{\parallel}V_{thi}$  (the electron cyclotron resonance is also plotted, but it lies expectedly out of the plotted frequency range).

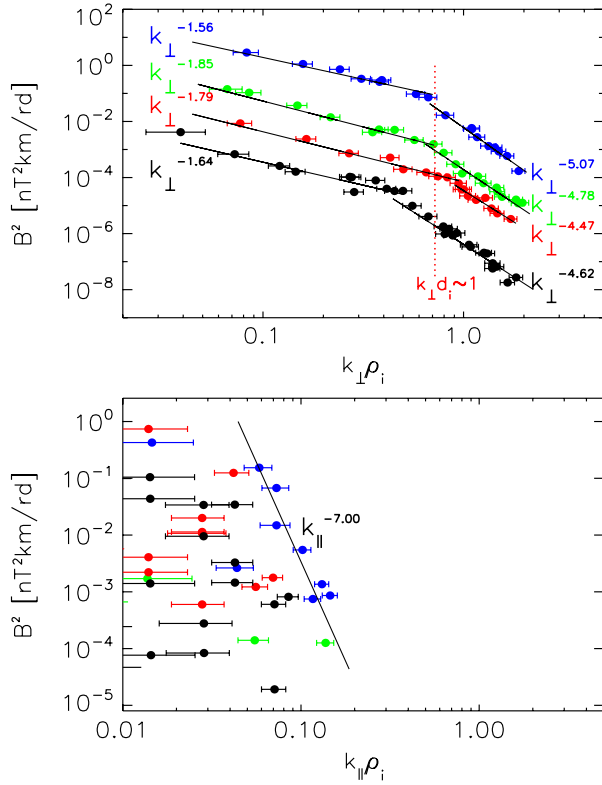


FIG. 6 (color online). Wave number spectra with estimated error bars for the four time intervals in the parallel (bottom) and perpendicular (top) directions to the local mean field. The vertical dotted line shows the proton inertial length.

to  $\mathbf{B}_0$ , while no cascade with a clear power law can be evidenced in the parallel direction. This may be due to significant uncertainties that affect the measurement of small values of  $k_{\parallel}$  as reflected by the error bars in Fig. 6 [21]. We found, furthermore, that the turbulence is slightly nonaxisymmetric (around  $\mathbf{B}_0$ ); the direction of anisotropy (not shown here) seems to correlate with  $\mathbf{V}_f$  as found previously by Refs. [5,18].

Figure 6 shows direct evidence that the breakpoint of the spectra occurs near the proton scale. While the spectra above the breakpoint follow the Kolmogorov scaling  $\sim k_{\perp}^{-1.7}$ , the spectra steepen to  $\sim k_{\perp}^{-4.5}$  below the breakpoint. This strong steepening combined with the dispersion curve of Fig. 5 suggests strongly that energy is transferred to protons via Landau damping. This may account for the temperature anisotropy  $T_{i\parallel} \sim 40 \text{ eV} > T_{i\perp} \sim 27 \text{ eV}$  observed during the four intervals of data studied here. It is clear from the spectra of Fig. 2, however, that not all the energy is transferred to protons; part of it “survives” the transition range and cascades down to smaller scales where it may be dissipated by electron Landau damping [7,9,12].

**Conclusions.**—We have shown the first 3D experimental dispersion relations and  $k$  spectra in the scale range  $[0.04, 2]k_{\perp\rho_i}$  in the SW and proved that the turbulence is carried by highly oblique KAWs. The  $k$  spectra were strongly anisotropic and showed a clear breakpoint near

the proton scale followed by a steeper spectrum  $k_{\perp}^{-4.5}$  than that predicted for the dispersive range by Refs. [12,32]. We suggested that in this transition range part of the energy is Landau damped into protons, while the remaining energy undergoes a dispersive cascade toward smaller scales where it may be dissipated into electron heating [7]. The anisotropy and scaling of the transition range observed here may be used to test theoretical models of wave-particle interactions near the proton gyroscale [22]. These observations can be applied to investigations of how astrophysical plasmas, such as the solar corona, are heated in the presence of turbulence.

The FGM and cluster ion spectrometry experiment data come from the CAA (ESA) and AMDA (CESR, France). We thank A. Viñas for providing the electron data. F. Sahraoui is funded partly by the NPP program at NASA/GSFC.

\*fouad.sahraoui@lpp.polytechnique.fr

- [1] W. H. Matthaeus and M. L. Goldstein, *J. Geophys. Res.* **87**, 6011 (1982).
- [2] S. D. Bale *et al.*, *Phys. Rev. Lett.* **94**, 215002 (2005).
- [3] L. Sorriso-Valvo *et al.*, *Phys. Rev. Lett.* **99**, 115001 (2007).
- [4] T. Horbury, M. Forman, and S. Oughton, *Phys. Rev. Lett.* **101**, 175005 (2008).
- [5] Y. Narita *et al.*, *Phys. Rev. Lett.* **104**, 171101 (2010).
- [6] C. P. Escoubet *et al.*, *The Cluster and Phoenix Missions* (Kluwer Academic, Dordrecht, 1995).
- [7] F. Sahraoui *et al.*, *Phys. Rev. Lett.* **102**, 231102 (2009).
- [8] K. Kiyani *et al.*, *Phys. Rev. Lett.* **103**, 075006 (2009).
- [9] O. Alexandrova *et al.*, *Phys. Rev. Lett.* **103**, 165003 (2009).
- [10] S. P. Gary and C. W. Smith, *J. Geophys. Res.* **114**, A12105 (2009).
- [11] J. J. Podesta *et al.*, *Astrophys. J.* **712**, 685 (2010).
- [12] A. Schekochihin *et al.*, *Astrophys. J. Suppl. Ser.* **182**, 310 (2009).
- [13] G. I. Taylor, *Proc. R. Soc. A* **164**, 476 (1938).
- [14] J.-L. Pinçon and F. Lefeuvre, *J. Geophys. Res.* **96**, 1789 (1991).
- [15] F. Sahraoui *et al.*, *J. Geophys. Res.* **108**, 1335 (2003).
- [16] F. Sahraoui *et al.*, *Ann. Geophys.* **22**, 2283 (2004).
- [17] B. Grison *et al.*, *Ann. Geophys.* **23**, 3699 (2005).
- [18] F. Sahraoui *et al.*, *Phys. Rev. Lett.* **96**, 075002 (2006).
- [19] Y. Narita *et al.*, *J. Geophys. Res.* **110**, A12215 (2005).
- [20] J. P. Eastwood *et al.*, *Phys. Rev. Lett.* **102**, 035001 (2009).
- [21] F. Sahraoui *et al.*, *J. Geophys. Res.* **115**, A04206 (2010).
- [22] G. G. Howes, *Phys. Plasmas* **15**, 055904 (2008).
- [23] R. J. Leamon *et al.*, *J. Geophys. Res.* **103**, 4775 (1998).
- [24] R. J. Leamon *et al.*, *J. Geophys. Res.* **104**, 22331 (1999).
- [25] M. L. Goldstein *et al.*, *J. Geophys. Res.* **99**, 11519 (1994).
- [26] R. J. Leamon *et al.*, *Astrophys. J.* **537**, 1054 (2000).
- [27] R. J. Leamon *et al.*, in *Solar Wind Nine: Proceedings of the 9th International Solar Wind Conference*, AIP Conf. Proc. No. 471 (AIP, New York, 1999), p. 469.
- [28] C. W. Smith *et al.*, *Astrophys. J.* **645**, L85 (2006).
- [29] T. Osman and T. Horbury, *Astrophys. J.* **654**, L103 (2007).
- [30] G. G. Howes, *Nonlinear Proc. Geophys.* **16**, 219 (2009).
- [31] G. G. Howes *et al.*, *J. Geophys. Res.* **113**, A05103 (2008).
- [32] S. Galtier, *Phys. Rev. E* **77**, 015302 (2008).